IOP Conference Series: Earth and Environmental Science

PAPER • **OPEN ACCESS**

Preparation of high-density fused quartz ceramics based on a J2-optimality mixed orthogonal method

To cite this article: Hou Qinglin *et al* 2019 *IOP Conf. Ser.: Earth Environ. Sci.* **233** 022009

View the article online for updates and enhancements.

This content was downloaded from IP address 218.240.53.53 on 08/10/2019 at 10:30

Preparation of high-density fused quartz ceramics based on a J_2-optimality mixed orthogonal method

Hou Qinglin[1], Wang Yingxia[1*], Tian Liang[1,2], You Yaoyao[1]

[1]School of Packing and Materials Engineering, Hunan University of Technology, Zhuzhou, 412008,P R China

[2]College of Chemical Engineering, Xiangtan University, Xiangtan, 411005, P R China;

the corresponding author's e-mail address: 625997280@qq.com

Abstract: A method for obtaining high-performance fused silica ceramics was investigated in this work. An advanced experimental method was used to prepare green bodies. The optimal experimental scheme was deduced using the hybrid orthogonal experiment method of J_2-optimality. The solid-phase content, the amount of dispersant, the pH and the milling time were used as variables. The effects of various factors related to the processing of fused silica ceramics on the performance of the crucible were studied. The structure and properties of the samples were characterized by using a universal testing machine, a scanning electron microscope, an electron density meter and an X-ray diffractometer. The results show that a solid-phase content of 65 wt%, a pH of 5, a dispersant content of 2.5 wt% and a milling time of 15 led to a green body with a flexural strength of 18.5 MPa and a bulk density of 1.91 g/cm^3, resulting in ceramics with improved mechanical properties.

1. Introduction

Like many other ceramic products, fused silica ceramics can not currently meet the requirements for use in a wide range of applications, however, fused silica ceramics show a strong potential for the development of ceramic materials. The preparation of fused silica ceramics by the traditional grouting moulding process leads to a lengthy production cycle and high production costs. Furthermore, the particles are segregated during the grouting process. The obtained green body exhibits layering especially in the case of large, thick-walled products, which leads to uneven structure and performance. Therefore, to meet the strength (bending strength greater than 40 MPa) and overall uniformity requirements of some special applications, the strength and uniformity of quartz ceramics must be improved to reduce the number of generated defects and increase reliability.

2. Experimental procedure

2.1 Materials preparation

In this work, the water-based gel system was selected with acrylamide (AM) as the monomer, *N*,*N*-methylenebisacryl (MBAM) as the crosslinking agent, and ammonium persulfate as the initiator.

In the initial stage of slurry preparation, HEMA and TMPTA were added to a certain amount of deionized water in a certain proportion. The fused silica powder was then mixed into a premix, the mixture was ball milled, and citric acid was added to adjust the pH. Finally, the appropriate amount of

Content from this work may be used under the terms of the Creative Commons Attribution 3.0 licence. Any further distribution of this work must maintain attribution to the author(s) and the title of the work, journal citation and DOI.
Published under licence by IOP Publishing Ltd

the dispersant was added. In the coagulation moulding process, the slurry was vacuum degassed and APS was added to the mould at room temperature; After drying, sintered samples were first degreased and then placed in a microwave sintering furnace. Different sintering temperatures and different heating rates were used; the sintering time was 3 h. The entire experimental process is shown in Fig.1:

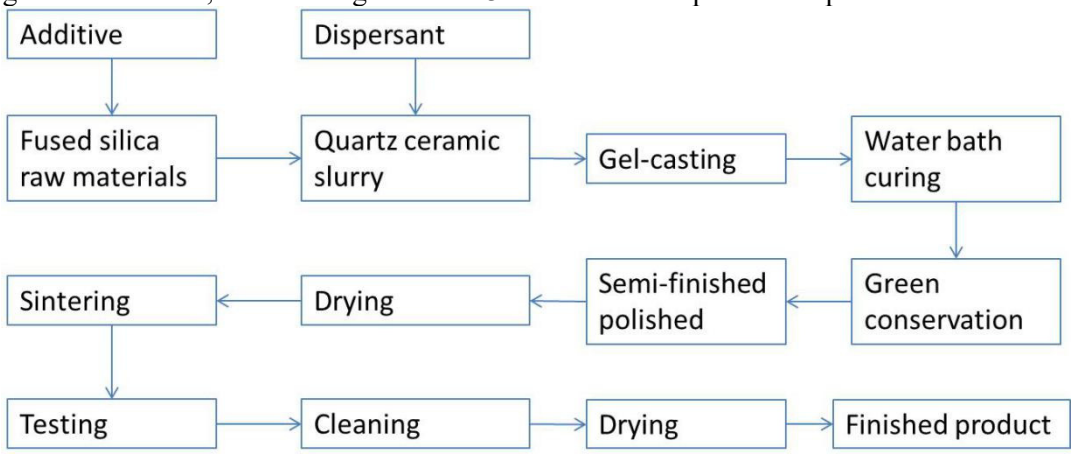


Fig.1 Flow chart of the gel-casting process

2.2 Testing method

Because of the unequal experimental effect of each factor, a reasonable orthogonal experiment scheme was obtained by optimizing the calculation according to an orthogonal experiment and the orthogonality,. The method used in this experiment is based on J_2-optimality hybrid orthogonal experiment, and the basic principle is described as:

$$O(x_i, x_j) = \frac{\sum_{k=1}^{m} \delta(x_{ik}, x_{jk})}{m} \quad (1)$$

where x_i and x_j are two rows in the experimental design (i.e., two experiments); m is the number of factors, and if $x = y$, then $\delta(x,y)=1$, otherwise, $\delta(x,y)=0$. Thus, the degree of similarity of the two experiments is evaluated.

The orthogonality of the entire experiment is defined as:

$$J_2(d) = \overline{O(x_i, x_j)} \qquad 1 \le i, j \le n \quad (2)$$

The solid-phase content, the pH , the amount of dispersant and the milling time were used as the influencing factors, and the viscosity of the slurry was used as the reference index. The factors and levels of the orthogonal test design were shown in Table 1. The orthogonal test scheme and the bulk density values of the samples are shown in Fig. 2, and the results of the orthogonal test are shown in Table 2.

Table 1. Orthogonal experimental factors and levels

Factor / Level	Solid content (wt%)	pH value	Amount of dispersant (wt%)	Milling time (h)
1	50	3	1.5	10
2	55	4	2.0	15
3	60	5	2.5	20
4	65	6	3.0	25

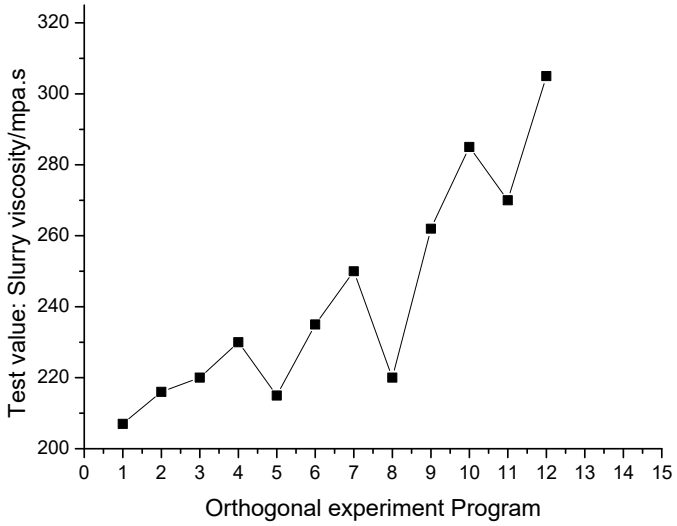


Fig.2 Orthogonal test scheme and measurement results

(1)Range method analysis
The results of the range method analysis are shown in Table 2:

Table 2. Results of the range method analysis

Factor	Factor A Solid-phase content（wt%）	Factor B pH value	Factor C Dispersant	Factor D Milling time (h)
$\sum 1/K_i$	14.33	43	43.75	40.5
$\sum 2/K_i$	26.67	30.25	37.75	45.5
$\sum 3/K_i$	44	55.5	47.25	42.75
$\sum 4/K_i$	86.67	/	/	/
R	72.34	25.25	9.5	5

R represents the range method, which is equal to the difference between the maximum and minimum values for each of the corresponding factors.

The results in Table 2 indicate that the order of significance of the orthogonal experiments is A, B, C, D(i.e.,solid content, pH value, dispersant, and milling time).A trend graph based on the magnitude of the Σ*i*/*Ki* values was constructed (Fig. 3) to enable a more intuitive selection of the optimal value of each factor:

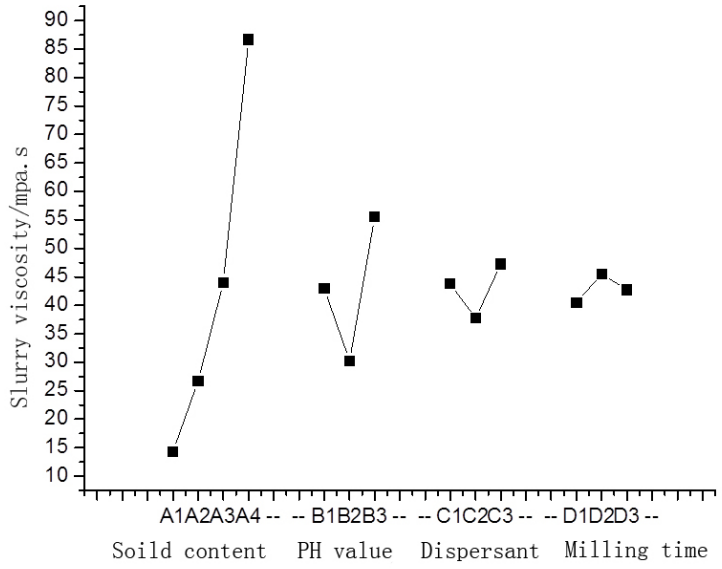


Fig.3 Analysis of orthogonal test results using the range method

(2) Variance method analysis

The results obtained using the orthogonal test calculation method are simple, intuitive and show a small range. However, the accuracy of the judgment effect is poor and the experimental error can-not be estimated. A large experimental error can lead to an inaccurate estimation, it often may cause miscarriage of justice. Therefore, we analysed the variance for validation after the analysis of the range method.

We first calculate the sum of squares prior to the variance analysis:

$$SS_T = \sum_{i=1}^{n} \left(T_i - \overline{T} \right)^2 \quad (3)$$

where $\overline{T}$ is the mean of all experiments; n is the total number of experiments; and T_i is the ith experimental value. We then calculate the square sum of the factor effects of A, B, C, and D factors: SS_A、SS_B、SS_C、SS_D:

$$SS_A = \sum_{i=1}^{L_A} k_{iA} \left(\frac{\sum_{iA}}{k_{iA}} - \overline{T} \right)^2 \quad (4)$$

After calculating the square of the factor effect of each factor, the error squared sum SS_e is calculated as follows:

$$SS_e = SS_T - SS_A - SS_B - SS_C - SS_D \quad (5)$$

where L_A is the number of levels of factor A; $\sum_{iA}$ is the sum of the experimental values at the level of factor A; k_{iA} is the number of experiments at the level of factor A.

After calculating the sum of squares of squares and SS_T and the effect of each factor, we can continue to calculate the mean square error and F test of each factor.

$$MSE_A = \frac{SS_A}{f} \quad (6)$$

$$F = \frac{MSE_A}{MSE_e} \quad (7)$$

Table 3. Results of the variance method analysis (1)

Source of variance	SS	f	MSE	F	Critical value	Significance
A	8988.9	3	2996.3	17.2	$F_{0.01}(2,2)=9$	(*)
B	1275.2	2	637.6	3.7	$F_{0.01}(3,2)=9$	/
C	184.7	2	92.3	0.5	$F_{0.05}(2,2)=1$	/
D	50.2	2	25.1	0.1	$F_{0.05}(3,2)=1$	/
MSE_e	348	2	174	/	/	/
T	10847	11	/	/	/	/

A comparison of the F values and the critical value does not indicate that they significantly influence each factor.The influence of A is largest, followed by (*) .To improve the accuracy of the analysis, we only considered the factor A because factors B, C, D are incorporated into the error.

Thus, $S_B + S_C + S_D + S_E$=1275.2+184.7+50.2+348=1858.1

Table 4. Results of the variance method analysis (2)

Source of variance	SS	f	MSE	F	Significance
A	8988.9	3	2996.3	12.89	(**)
MSE'_e	1858.1	8	232.3	/	
T	10847	11	/	/	/

$F_{0.05}(3,8)=9.6$； $F_{0.01}(3,8)=7.59$

A comparison of the *F* value and the critical value reveals that factor A is the significant factor. In this case, the order of influence is ABCD, and the selected optimal scheme should be $A_4B_3C_3D_2$. That is, the solid-phase content, pH, amount of dispersant, and the milling time should be 65%, 5, t 2.5%, 15 h respectively.

On the basis of these two methods—the range method and the variance method—we observe that the four factors have a certain influence on the green body density with the solid-phase content having the greatest influence on the density of the green body, followed by the pH and the dispersant content, and with the milling time having the smallest effect; This order of influence of the factors is attributed to the density of ceramic materials and the solid-phase content of their slurry being closely related. To ensure high strength of the body minimize product shrinkage, and avoid deformation, cracking and other defects, the experimental program should be designed to improve the slurry solid-phase content of the powder as much as possible; We deduced that the optimum conditions are: a solid-phase content of 65 wt%,a pH equal to 5, a dispersant content of 2.5 wt% and a milling time of 15 h.

3. Results and discussion

3.1 Scanning electron microscopy analysis

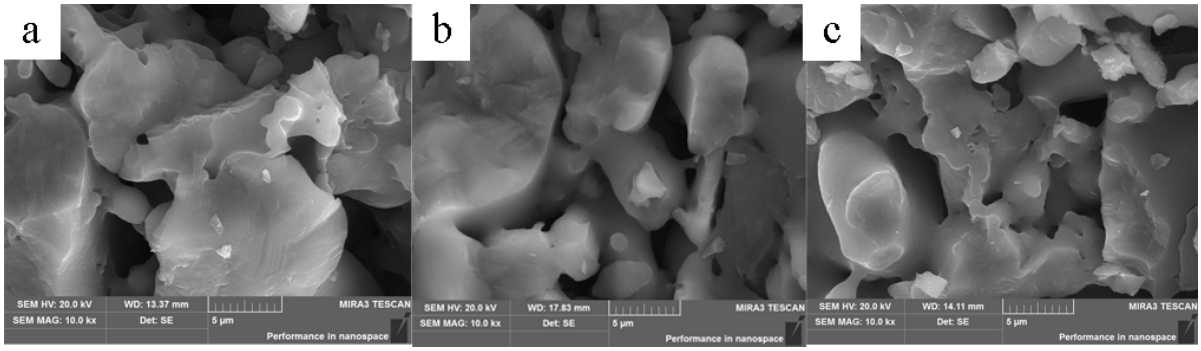


Fig. 4 SEM images of samples with different solid-phase contents: (a):55%, (b):60%, and (c):65%.

It can be seen from Figure c, when the solid content of 65%, the sample appeared a lot of larger particles. This shows that in this case there is a liquid phase, the product particles in close contact between the sintering densification uniform,While the other two groups of particles are not close, more pores, so that the strength of burning products, hardness are affected.

3.2 X-Ray Diffraction analysis

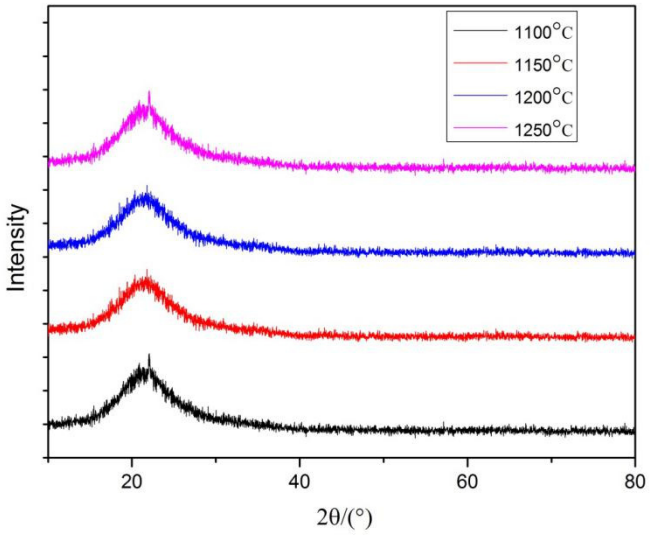


Fig.5 XRD with different sintering temperature

It can be concluded from Fig. 4 that the crystallization peak of the fused silica ceramic sample is not much different when the sintering temperature is at 1150 ℃ and 1200 ℃, and there is not much crystal quartz. But the sintering temperature rose to 1250 ℃, the square quartz crystal peak is more obvious, and it will affect the use of fired products performance. Under these conditions, the optimum sintering temperature was chosen to be 1200℃.

3.3 Flexural strength test

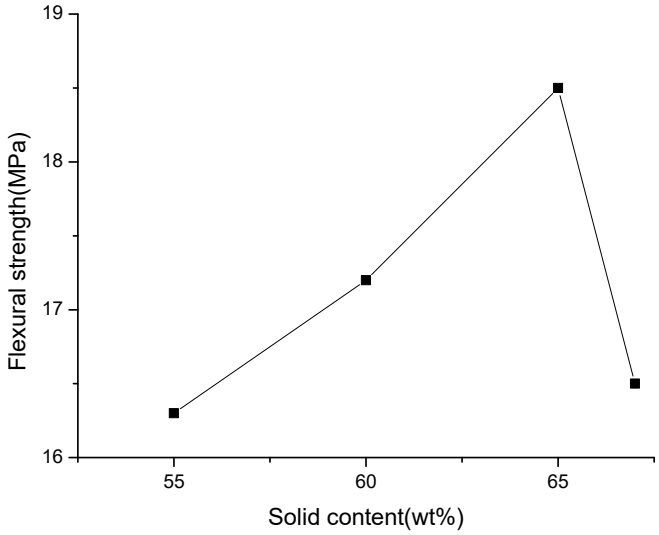


Fig.6 The relationship between the flexural strength and the solid content

With the increase of the solid content, the flexural strength of the green body first increases, and reaches the highest value when the solid content is 65%, and then decreases. The reason for this is that the strength of the green body is improved and the strength of the green body is enhanced as the solid content increases. However, as the solid content is further increased, the total amount of liquid to be adsorbed increases and the free-flowing liquid becomes less. At the same time, the distance between the particles in the slurry becomes smaller, the organic chains adsorbed on the surface of the particles are overlapped with each other, so that the movement between the particles is difficult and the flow ability is deteriorated. These are not conducive to the slurry removal and pouring molding, so the intensity decreases.

4. Conclusion

There are many influencing factors of coagulation molding process, and the previous experiments are based on single factor optimization experiment method, control variables to arrange the experiment, making the experimental workload is heavy and heavy. In this experiment, the orthogonal experiment was designed to obtain the parameters of high solid phase and low viscosity slurry. The solid phase content, pH value, dispersant dosage and milling time were used as influencing factors.

Acknowledgements

We would like to acknowledge the National Natural Science Foundation of China（51374103）, the National Natural Science Foundation of China（51674114）,and the National Natural Science Foundation of China（51174085）for financial support.

Reference

[1] Amkreutz D, Haschke J, Häring T, et al. Conversion efficiency and process stability improvement of electron beam crystallized thin film silicon solar cells on glass[J]. Solar Energy Materials and Solar Cells, 2014, 123: 13-16.
[2] Green M A, Emery K, Hishikawa Y, et al. Solar cell efficiency tables (Version45)[J]. Progress in photovoltaics: research and applications, 2015, 23(1): 1-9.
[3] Branker K, Pathak M J M, Pearce J M. A review of solar photovoltaic levelized cost of electricity [J]. Renewable and Sustainable Energy Reviews, 2011, 15(9): 4470-4482.
[4] Miles R W, Hynes K M, Forbes I. Photovoltaic solar cells: An overview of state-of-the-art cell

development and environmental issues[J].Progress in Crystal Growth and Characterization of Materials,2005,51(1-3):1-42.
[5] Liu S H, Chen P, Xu D H, et al. Effects of Sintering Temperature on Phases, Microstructures and Properties of Fused Silica Ceramics[C].Key Engineering Materials. Trans Tech Publications, 2017, 726: 399-403.
[6] Porozova S E. Optimized composition of the slip for preparing high-porosity permeable quartz ceramics[J].Refractories and industrial ceramics, 2002, 43(7): 269-272.
[7] German R M. Powder injection molding-design and applications[M].Pennsylva-nia:IMS Inc,2003.
[8] Jenny M A, Omalete O O. Method for molding ceramic powders using a water-based gel casting process: U.S. Patent 5,145,908[P]. 1992-9-8.
[9] Bude J, Miller P, Baxamusa S, et al. High fluence laser damage precursors and their mitigation in fused silica[J]. Optics express, 2014, 22(5): 5839-5851.
[10] Cai K, Huang Y, Yang J. A Synergistic Low‐Toxicity Gelcasting System by Using HEMA and PVP[J]. Journal of the American Ceramic Society, 2005, 88(12): 3332-3337.
[11] Cai K, Huang Y, Yang J. Alumina gelcasting by using HEMA system [J]. Journal of the European Ceramic Society, 2005, 25(7): 1089-1093.
[12] Chen B, Zhang Z, Zhang J, et al. Aqueous gel-casting of hydroxyapatite[J]. Materials Science and Engineering: A, 2006, 435: 198-203.
[13] Omatete O O,Nick J. Improved gelcasting systems[J]. Ceram Eng. Sci Proc,1999, 20(3):241- 248.
[14] Tari G.Gelcating ceramics: a review[J]. Am Ceram Bull, 2003, 82(4):43.
[15] Adolfsson E. Gelcasting of zirconia using agarose[J]. Journal of the American Ceramic Society, 2006, 89(6): 1897-1902.
[16] Xu H, Liu J, Guo A, et al. Porous silica ceramics with relatively high strength and novel bi-modal pore structure prepared by a TBA-based gel-casting method[J]. Ceramics International, 2012, 38(2): 1725-1729.
[17] Hu Y, Wang Z, Lu J. Study on the gel casting of fused silica glass[J]. Journal of Non-Crystalline Solids, 2008, 354(12): 1285-1289.
[18] Netz D J A, Sepulveda P, Pandolfelli V C, et al. Potential use of gelcasting hydroxyapatite porous ceramic as an implantable drug delivery system[J]. International journal of pharmaceutics, 2001, 213(1): 117-125.
[19] Zbigniew S. Advanced shaping techniques in advanced ceramics [J]. Cfi/Ber DKG, 2000, 77 (6): 6-16.